

Irreversible modifications of the porous microstructure of soluble anhydrite β -CaSO₄ induced by hydration-dehydration cycles

Pierre BRACCONI*, Jean-Claude MUTIN

Laboratoire Interdisciplinaire Carnot de Bourgogne, UMR 5209 CNRS,

Université de Bourgogne, BP 47870, F-21078 Dijon, France

*corresponding author

Tel. : + 33 (0)380 396 154. / Fax : + 33 (0)380 393 819

e-mail : pierre.bracconi@u-bourgogne.fr

Abstract

The internal surface area of hexagonal (soluble) primary anhydrite CaSO_4 produced by dehydration of gypsum decreases by about 70 % when the anhydrite is successively subjected to rehydration and dehydration at room temperature in humid air and in vacuum respectively. In the rehydration step, the hemihydrate is formed; its dehydration yields secondary anhydrite. Additional hydration-dehydration cycles in the same conditions have a much smaller effect. The first cycle also brings about a modification of the t-plot, which reveals that the micropores of primary anhydrite are irreversibly healed. Mercury intrusion porosimetry shows that the primary dehydration of gypsum also generates an open porosity of 25-28% comprised of macro and mesopores with opening width ranging over 5 decades. The distribution of the finest mesopores only is slightly modified by subsequent hydration-dehydration cycles. The initial external volume of the gypsum crystals remains essentially unchanged throughout the successive reaction cycles (i.e. the pseudomorphs undergo neither swelling nor shrinkage).

Keywords

Gypsum; Anhydrite; Surface area; Porosity

1. Introduction

The dehydration of gypsum at moderate temperature is a topotactic reaction [1, 2] that can lead either to the hemihydrate $\text{CaSO}_4 \cdot 0.5\text{H}_2\text{O}$ (noted $\text{HH}_{0.5}$), or to the anhydrite CaSO_4 , depending on temperature and humidity conditions. The hemihydrate prepared in that way is referred to as $\beta\text{-HH}_{0.5}$ in contrast with $\alpha\text{-HH}_{0.5}$ prepared in hydrothermal conditions and that exhibits a different microstructure. At high humidity level, typically >45-50% RH at room temperature, the crystal structure is modified to incorporate additional water molecules according to the composition $\text{CaSO}_4 \cdot 0.6\text{H}_2\text{O}$ [3] (noted $\text{HH}_{0.6}$). Multilayer adsorption of water vapour on the surface can notably increase the overall water content of these phases beyond their structural water content. The anhydrous phase can exist either as soluble anhydrite, noted A3, or insoluble anhydrite, noted A2. In any case, the dehydration product ($\beta\text{-HH}_{0.5}$, A3 or A2) exhibits a porous microstructure and is referred to as a pseudomorph. As confirmed by the present work, its porosity makes up more or less quantitatively for the difference between the molar volumes of the initial and final solid phases. The change of structure results in the formation of cracks with defined crystallographic orientations and broadly distributed width and length as readily observed on the outer surface of the pseudomorphs [1, 2].

The internal surface area and pore volume of porous solids are classically characterized by vapour adsorption and mercury intrusion porosimetry (MIP), but to the authors' knowledge, no quantitative description of the microstructure of any of the pseudomorphs using MIP has ever been reported. More or less fragmentary vapour adsorption data only can be found in the literature. Ball and Norwood [4-6] investigated the microstructure of dehydrated gypsum and dehydrated hemihydrate ($\alpha\text{-HH}$ and $\beta\text{-HH}$) by nitrogen adsorption. Molony et al [7-9] compared the adsorption isotherms of nitrogen and oxygen vapours on more or less similar materials and investigated the effect of successive dehydration-rehydration of the hemihydrate. The BET surface area and the adsorption-

desorption hysteresis loop differ widely from one adsorbate to the other. In all above mentioned investigations, the initial gypsum samples were dehydrated under ambient air at temperatures in the range 100-200°C air, and subsequently converted to β -HH at room temperature. However, the exact phase composition and water content of the hemihydrate samples *in the conditions of the nitrogen adsorption experiments* were unclear. Hamad [10] also observed the gradual decrease of the BET surface area of one sample of β -A3 following successive *partial* rehydration-dehydration cycles. Rehydration was obtained by exposure to an atmosphere *saturated* with water during increasing laps of time and the surface area measurements were carried out after dehydration in the same conditions as with the initial gypsum sample, namely 100°C under vacuum. The surface area, initially equal to 23,40 m².g⁻¹, reached the ultimate value of 0.96 m².g⁻¹ after 15 days of accumulated treatments. All starting materials in [4-10] consisted of gypsum or α -hemihydrate *powders* whose external surface area contributed to the measured pseudomorph surface area in unknown proportions.

The experimental results presented in the following contribute to a significant improvement in the quantitative description of the microstructure of the pseudomorphs. This was achieved firstly by investigating the dehydration products of cleft lumps of natural gypsum instead of powders produced by comminution or precipitation and secondly by performing nitrogen adsorption and MIP experiments sequentially on the same samples or on fractions of them. In such conditions, the contribution of the initial surface area of a lump to the total surface area of the pseudomorph is practically nil, and adsorption experiments provide direct unbiased information on the *internal* surface area generated by the reaction. As for MIP, the complications arising from the compression of the powder bed and filling of its bulk porosity (that can represent the major part of the overall intrusion [1]) are eliminated, and the intrusion curve specifically characterises the internal porosity of the pseudomorph.

The direct characterisation of the actual microstructure of HH using nitrogen adsorption and MIP has not been attempted for obvious reasons: the microstructure strongly depends on water content and the hemihydrate loses water under vacuum at room temperature. This is incompatible with the (temporary) vacuum conditions required by both techniques.

Lastly, particular efforts were devoted to controlling the solid phase water content in all analytical conditions and to identifying and evaluating the error associated to the various measured quantities.

2. Experimental

The starting material consisted of small lumps cleft from a large block of natural gypsum. Its transparency was evidence of a high purity level. The concentrations of calcium and sulphate ions in a small sample were measured by IPCMS. They departed very slightly from the theoretical values expected for pure stoichiometric calcium sulphate dihydrate, by +0.18% and -1.36% respectively, and the molar calcium-sulphate ratio was found equal to 1.015.

A cleft gypsum lump is limited by three types of crystallographic faces, parallel to the three natural cleavage planes of the crystal structure, (010), (011) and (100) [11]. Faces parallel to the principal (easy) cleavage plane (010) are made of large terraces and ledges with no cracks visible at any scale. In contrast, faces parallel to the secondary fibrous cleavage plane (011) exhibit relatively large cracks limited by exfoliated (010) planes. This is the result of shearing during cleaving. Depending on the thickness of a lump along the [010] direction, faces parallel to (010) and (011) planes will have different extents. Accordingly, the number and internal volume of such cracks present prior to dehydration is changing from one crystal to another. Analysis by MIP proved that their widths remain larger than about one micron and their cumulated internal volume can be regarded as negligibly small in the following. In

contrast, the dehydration itself generates cracks emerging on all faces and characterised by a broad distribution of width as described in [1, 2].

First, A3 samples were produced by dehydration of about 1g of cleft gypsum lumps under high (turbomolecular) vacuum, at temperatures in the range 100-200°C. In the following, this step is referred to as primary dehydration and its product as *primary anhydrite* noted A3P. Slow heating, at 6°C per hour, and a long isothermal plateau of 15 hours were imposed, ensuring complete dehydration and a stable homogeneous final microstructure. After cooling to room temperature (RT) under vacuum the nitrogen adsorption isotherm of the pseudomorph so formed was measured using the Autosorb® from Quantachrome. Complementary measurements were also carried out using the other following instruments: Autosorb-1C® , ASAP® 2010 from Micromeritics or the Belsorp-Mini® from Bell Co. Next, the samples were subjected to one or several cycles of hydration (to form the hemihydrate) and dehydration (to return to the A3 phase). These two successive reactions were carried out at RT, in ambient air (25-35%RH) and under high vacuum respectively. In the following, they are referred to as one H-D cycle and the obtained product as *secondary anhydrite* noted A3S. In several cases, the porosity of a *fraction* of the sample utilised in the adsorption experiment was carried-out by MIP, with the help of the Autopore III® from Micromeritics. The anhydrite samples were handled and transferred under dry atmosphere following a strict experimental procedure as explained now.

All dehydration and hydration reactions were carried out with the solid sample contained in the same glass cell (a bulb with a long stem) used to perform the nitrogen adsorption experiment on the Autosorb (or other equipment). Starting from a known mass of gypsum, the composition of the product phase (either A3 or HH) was verified at each step by weighing the closed glass cell containing the reaction product. For dehydration, the cell was placed in a reaction chamber connected to the turbo-molecular pumping unit and heated by an external furnace. After reaction and return to RT the reaction chamber was filled up with pure

nitrogen. Then the cell was removed and the open end of the stem blocked with a rubber cork within seconds. After weighing, it was installed on the adsorption port of the Autosorb and immediately evacuated. Such conditions preclude the possibility for the anhydrite to react with water vapour as proved by the following observation. If the cell containing the anhydrite was uncorked and placed on the plate an analytical balance, its weight remained unchanged for tens of minutes, before water vapour could diffuse to and start reacting slowly with the anhydrite. In contrast, if fresh air was forced to circulate within the bulb through a capillary inserted in the stem, complete reaction took place within a few hours and this is how all rehydrations were carried out.

In order to perform a MIP experiment, a fraction of the A3 sample had to be introduced into the penetrometer without exposure to ambient water vapour. This was done in a glove box under dry air with the open end of the capillary of the penetrometer sealed with a removable plug. The overall assembly could thus be carefully weighed and the A3 sample weight precisely known. Finally, the penetrometer was installed onto the port of the porosimeter within seconds and evacuation was started immediately.

As regard the correction of the porograms (mercury intrusion curves), the subtraction of a blank experimental file proved more reliable at the highest pressures than the correction formula provided with the instrument software from Micromeritics (this point is illustrated in the result section). The blank experiments were carried out with various loads of non-porous stainless steel balls in the same analytical conditions as used for the anhydrite samples. The average and standard deviation of 3 or 4 such experiments was computed for each stainless steel sample volume. Finally, the intrusion curves of the anhydrite samples were corrected by subtracting the average blank curve of the stainless steel sample with the same or nearest volume. It must be understood that the influence of the compressibility of the non-intruded fraction of a *porous* sample on the measured porogram cannot be corrected for by a blank experiment. The standard deviation of the blank curves increases steadily with increasing

applied pressure. The *highest* observed value was about 0.0035 cm^3 . Assuming a similar standard deviation would be obtained if experiments with a A3 or HH sample could be repeated, one may estimate that the experimental error on pore volumes measured at the highest pressure (400MPa) is lower than about $\pm 0.007 \text{ cm}^3$.

Pressures values have been converted into width of slit-shaped pores, E , using Washburn equation $E = -2\gamma \cos \theta / P$ with $\theta = 130^\circ$, and $\gamma = 0.484 \text{ J.m}^{-2}$.

TGA experiments have been carried out using a precision microbalance (MTB10-8 from Setaram). The crystal structure of the hemihydrate has been checked by X-ray diffraction in air with Cu-K α radiation.

3. Results

The A3 pseudomorphs are known to react reversibly with water vapour in ambient conditions [12]. This is confirmed by the TGA curves shown in **Fig.1**. The isothermal water up-take of a secondary anhydrite sample exposed to ambient air with 25-35 %RH amounted to $0.60 (\pm 0.02)$ mole H_2O per mole CaSO_4 . The uncertainty is due to the fact that the origin of the gravimetric signal is evaluated by extrapolating the weight-vs-time curve to zero time, t_0 , defined as the moment the sample was dropped from the Autosorb cell onto the pan of the microbalance. When exposed to vacuum, the hemihydrate sample lost water following curve b of **Fig.1**.

In contrast with the hydration step, the final stage of dehydration is very slow. The final weight loss, calculated by extrapolating the TGA trace at infinite time, was found in the range 0.58 - 0.60 mole H_2O per mole CaSO_4 .

Depending on the humidity level during analysis, the powder X-ray diffractogram of the HH phase recorded in ambient conditions may be found in accordance with the crystal structure of either $\text{HH}_{0.5}$, or $\text{HH}_{0.6}$. Though the distinction between both is delicate and an excess of water with respect to the stoichiometry $\text{CaSO}_4 \cdot 0.5\text{H}_2\text{O}$ may be due to multilayer adsorption on the

surface and to a mixture of both phases. This is the reason why the relation between water content and structure of our hemihydrate samples was not investigated.

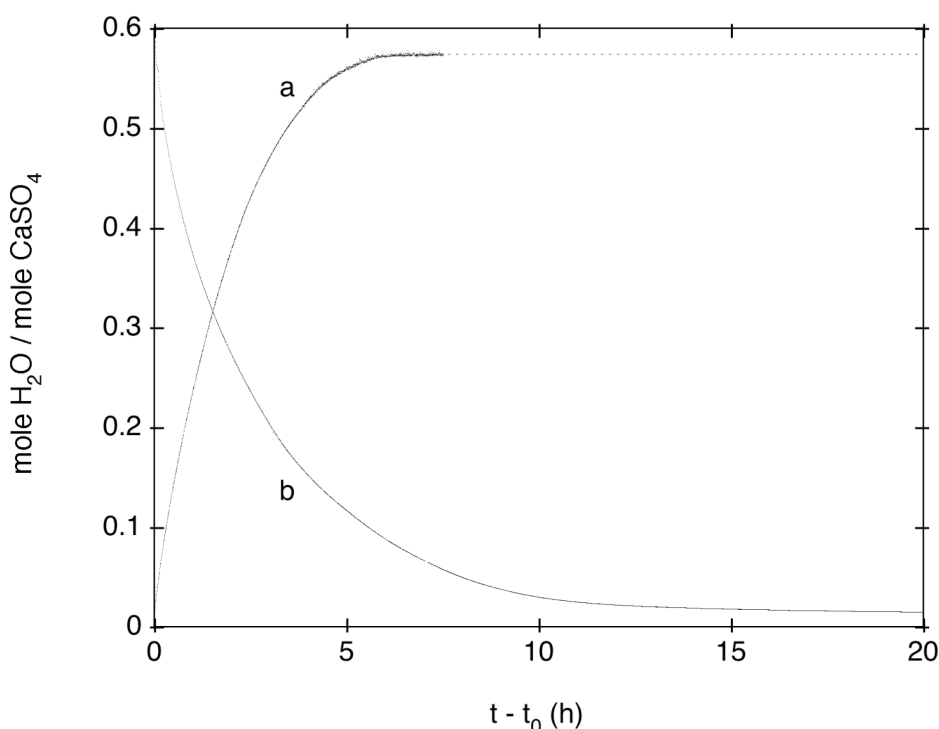


Fig.1: TGA of the hydration (curve a) and dehydration (curve b) of A3S at RT.

Nitrogen adsorption

All nitrogen adsorption isotherms of primary and secondary anhydrite (**Fig.2**) were of type II in the IUPAC classification [13] with high values of the C constant. BET surface area (S_{BET}) values between 19.3 and 20.2 m²g⁻¹ were obtained for A3P dehydrated at temperatures ranging from 98.5 to 199°C . These results are compared with literature data in the appendix. The desorption branch reveals a narrow hysteresis loop of H3 type [13] and some low pressure hysteresis. The intensity of low pressure hysteresis varied significantly with the instrument used (it proved the lowest with the Belsorp-Mini®, the largest with the ASAP2000®) but was always present. In comparison, low pressure hysteresis is not observed in the A3S isotherms.

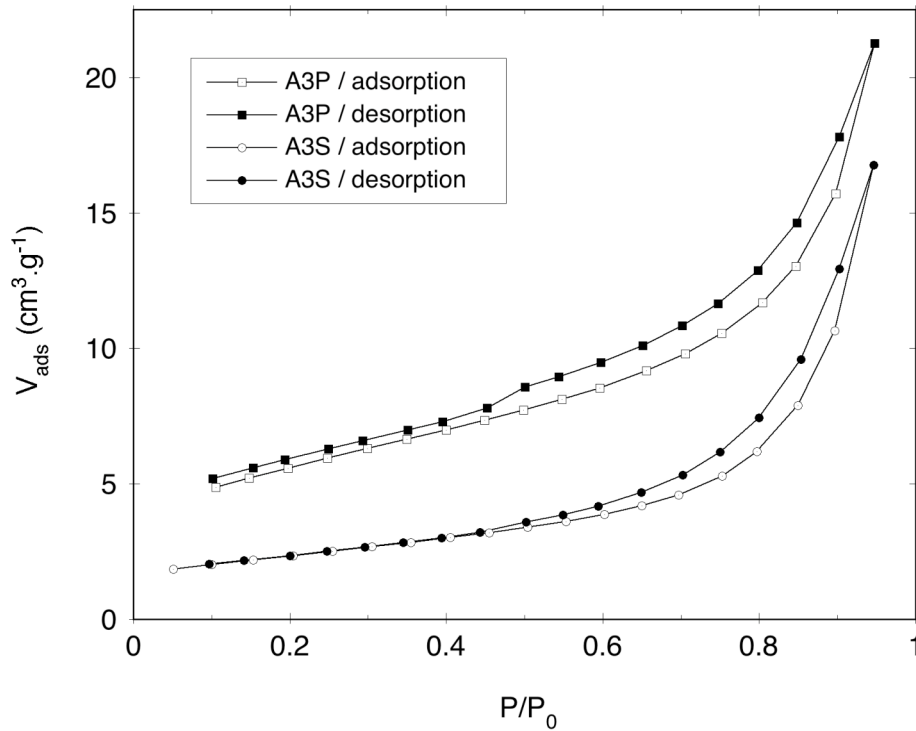


Fig.2: Nitrogen adsorption-desorption isotherm of one A3P sample obtained by dehydration of gypsum at 125 °C and of the same sample after one HD cycle. The Autosorb® 1C was used for the measurements.

The influence of successive H-D cycles on the BET surface area is shown in **Fig.3**. The first H-D cycle brought about a large drop of 70%, down to $5.9 (\pm 0.3) \text{ m}^2\text{g}^{-1}$ whereas subsequent cycles had much smaller effects. The final overall decrease after 3 cycles reached 77%. Prior to surface area measurement, the HH samples were dehydrated under vacuum *at room temperature* only i.e. not thermally degassed, the usual practice in adsorption experiments. That procedure was intended to ensure strictly identical sample preparation conditions for the adsorption and mercury porosimetry experiments since thermal degassing is impracticable in the mercury porosimeter. It is validated by the fact that quantitative dehydration of the hemihydrate phase (loss of its structural water) was systematically obtained at RT by overnight turbomolecular pumping and that the secondary anhydrite samples were not re-exposed to air prior to nitrogen adsorption. Nevertheless, two tests were performed to evaluate its possible influence on the measured area values. When adsorption

was duplicated after an intermediate degassing at 100°C a small increase of the BET surface area could be observed, equal to 0.15 and 0.20 m².g⁻¹ respectively. This is sufficiently small compared to the area reduction resulting from the first H-D cycle so as not to bias the final conclusions.

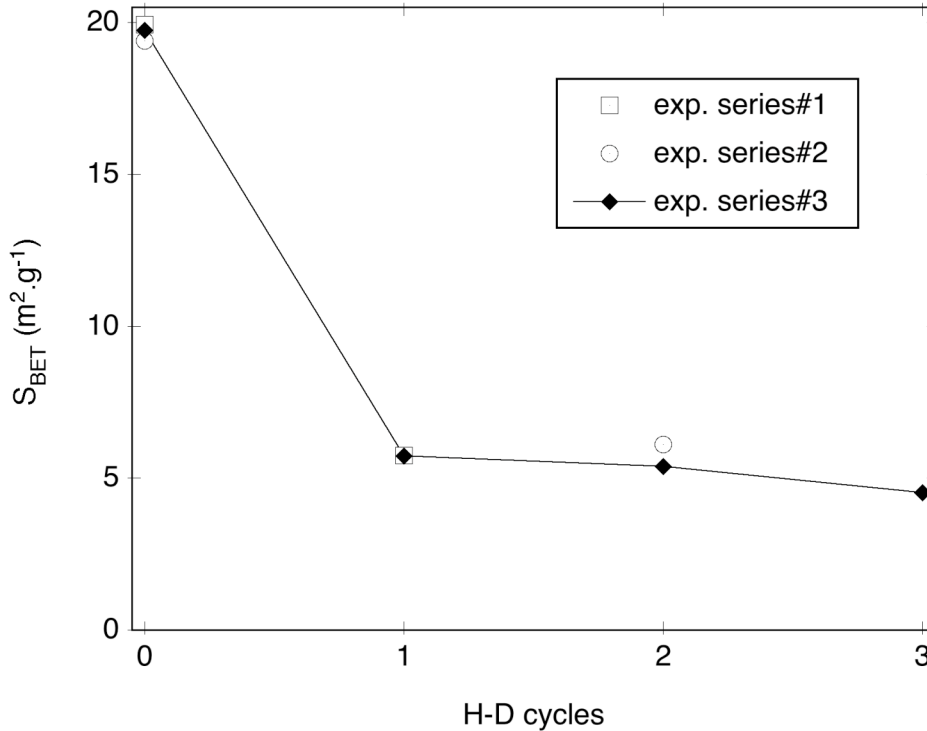


Fig.3 : BET surface area of primary and secondary anhydrite as a function of the number of H-D cycles. The Autosorb[®] was used for all measurements.

The first H-D cycle also brings about a modification in the t-plot of the adsorption branch of the isotherm. This is illustrated in **Fig.4** which is based on the results of a single experiment involving 3 successive H-D cycles but is fully representative of all others (by dividing the adsorbed volume by the BET monolayer capacity V_m , it was observed the adsorption isotherms of all five A3P samples could be superimposed in a reduced t-plot $V/V_m - vs - t$ not shown). The t-plots of A3P systematically revealed the presence of micropores and the micropore surface area, S_{MP} , was found to range from 5.1 to 5.9 m².g⁻¹ i.e. 27.7 (±1.0) % of S_{BET} on the average. The micropore volume (expressed in volume of liquid

nitrogen) ranged from 0.0023 to 0.0029 $\text{cm}^3 \cdot \text{g}^{-1}$, that is less than 2% of the total volume of macropores and mesopores measured by MIP (see below). The external surface area (i.e. of all mesopores and macropores) was found equal to 14.0-14.6 $\text{m}^2 \cdot \text{g}^{-1}$. In contrast the t-plots of A3S indicate that micropores are no longer present at least at a measurable level (lower adsorbed volumes entail lower accuracy). They also exhibit a sharper convexity at $t > 1.5$ nm.

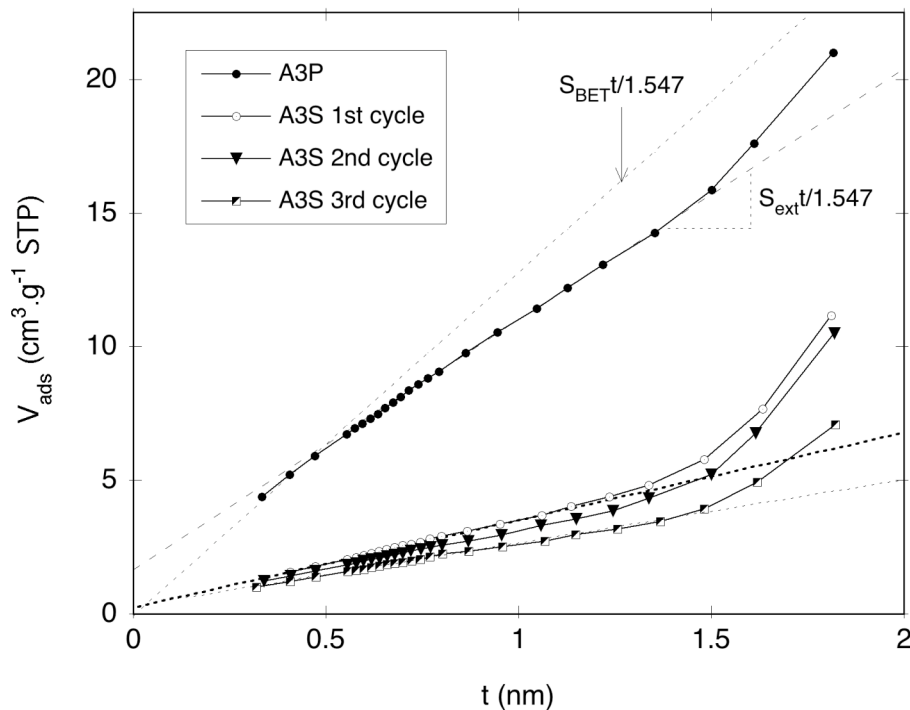


Fig.4: t-plots calculated from the adsorption isotherms of primary and secondary anhydrite over a series of three consecutive H-D cycles.

Mercury intrusion porosimetry

Except where otherwise stated, all numerical results derived from MIP were obtained from programs corrected for the blank according to the file subtraction procedure detailed in the experimental section. They are summarized in **Tab.1**.

The apparent (bulk) specific volumes, $V_{a,sp}$, of the various samples of primary and secondary anhydrite were systematically measured and their respective arithmetic means (first row of **Tab.1**) differ by 0.008 $\text{cm}^3 \cdot \text{g}^{-1}$, that is 3-4 times less than the standard deviation on

each individual mean. That such a difference is not statistically significant may be proved by noting that the standard error for the difference between the means is found equal to 0.018 whereas a value lower than 0.003 would be required in order to validate the hypothesis that the two means are different with a 95% confidence level. The same can be said of the specific pore volume, $V_{p,sp}$, and of the *open* porosity that remained practically unchanged around 26% through successive cycles. The density, ρ , of the solid phase can then be computed by $\rho = 1/(V_{a,sp} - V_{p,sp})$. In all cases but two, its value was found lower than the theoretical value inferred from structural parameters ($\rho_{X-ray} = 2.556\text{g}\cdot\text{cm}^{-3}$). In principle, this may be explained by the occurrence of closed porosity and the later was estimated at 5 and 7 % for A3P and A3S respectively. Though, the uncertainty on these last figures is very high and additional evidence would be desirable to ascertain the existence of closed pores.

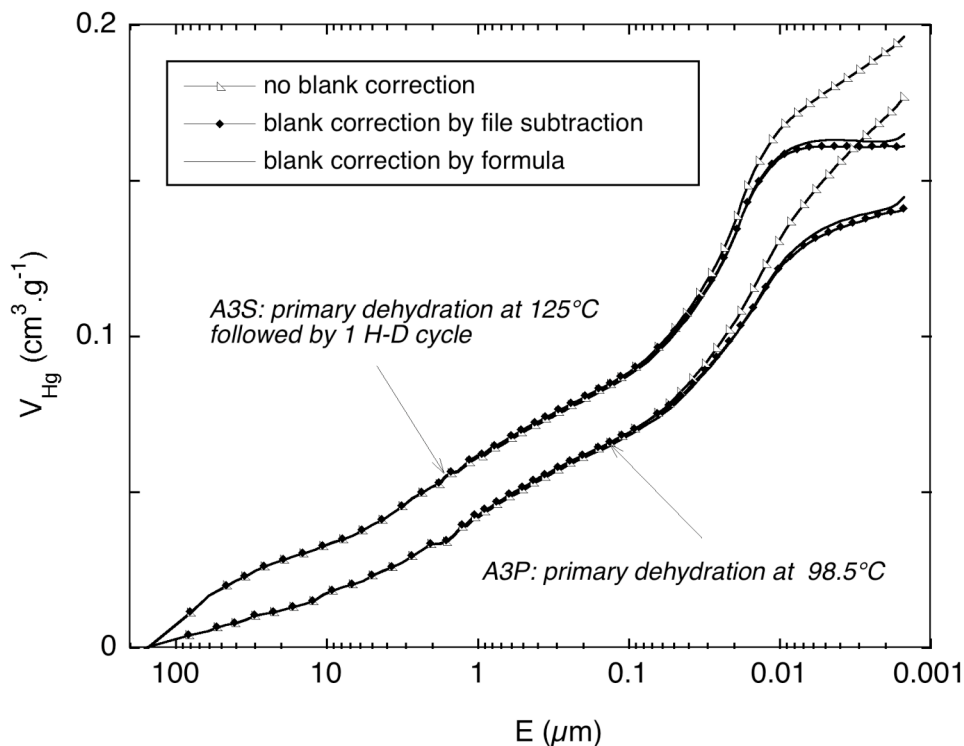


Fig.5: Porograms of one primary and one secondary anhydrite sample. In each case the raw intrusion curve is compared to the curves corrected for blank by blank file subtraction and by using the Micromeretics correction formula.

As a complement to **Tab.1**, the mercury intrusion curves in one A3P sample and one A3S sample are compared in **Fig. 5**. In each case, the raw (uncorrected) experimental curve and the curves corrected for blank by formula and by file subtraction are shown. The better performance of the latter is demonstrated by the removal of the very short final upward tail below $E \approx 0.002 \mu\text{m}$ that is present in the curves corrected by formula and is responsible for physically inconsistent (excessively large) surface area values (S_{MIP} defined further below).

As just mentioned above, the *average* open porosity (volume of open pores) is not significantly modified by H-D cycles (**Tab.1**). This is in apparent contradiction only with the shift between the two intrusion curves shown in **Fig.5**. The difference between the total open porosity values in these particular experiments is just equal to the sum of the standard deviations on $V_{p,sp}$ appearing in **Tab.1**. Those particular two curves were selected to emphasise the fact that the different *initial* slopes of the porograms around $E = 100 \mu\text{m}$ is the *major source of dispersion of the final values of $V_{p,sp}$* reflected in their standard deviation. As explained in section 1, the number of large slits initially present in cleft gypsum lumps and consequently in their pseudomorphs is variable independently of the dehydration reaction. Next, when pressure is increased, the two curves in **Fig.5** are running essentially “parallel” over a broad range of E values, typically from 20 to $0.1 \mu\text{m}$. As a consequence, the corresponding sections of the volume based pore size distributions (PSD) for primary and secondary A3 are simply indistinguishable.

The noticeable point when comparing the final section of the corrected porograms of A3P and A3S samples is that the later reach a plateau at pressures corresponding to mesopores with openings lower than $0.006\text{-}0.007 \mu\text{m}$ (**Fig.5**). The conclusion that can be safely drawn is that the narrowest mesopores (or their most part) are healed in the first H-D cycle along with the micropores, as revealed by the modification of the t-plots .

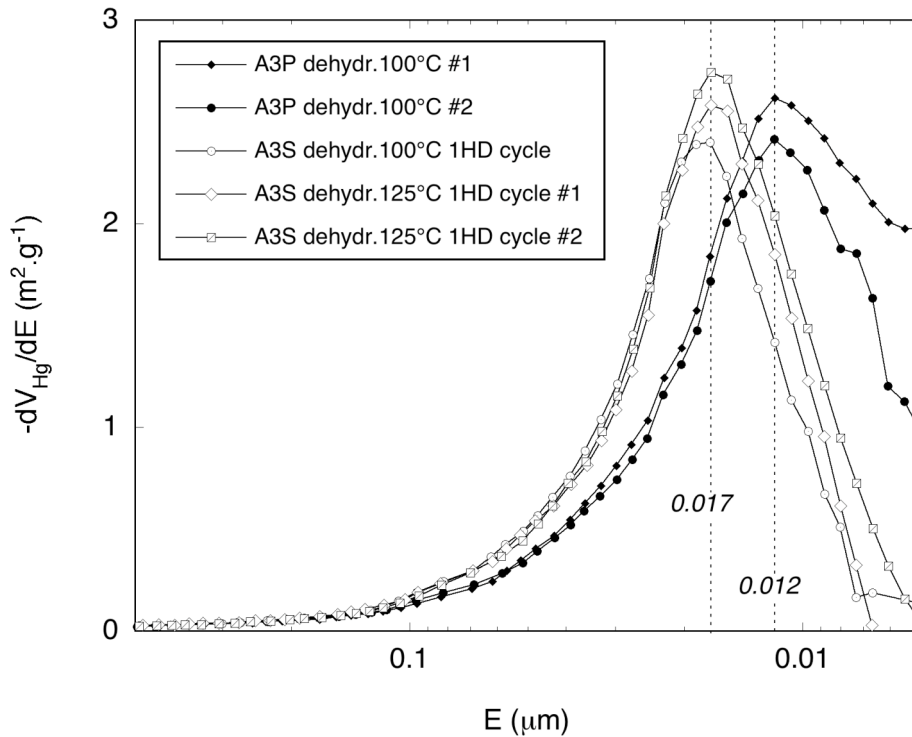


Fig.6: Comparison of the differential porograms, $-dV_{Hg}/dE$ of A3P and A3S samples. Assuming slit shaped pores with parallel faces, the curves represent the volume based distribution function of slit width E . The major modes are at $0.012\mu\text{m}$ and $0.017\mu\text{m}$ for A3P and A3S respectively.

Some physically inconsistent (negative) values of the PSD of the A3S samples may be obtained in the range $0.006\text{-}0.003\mu\text{m}$, but this clearly is in relation with the limited accuracy of the intrusion measurement and blank corrections at the highest pressures (the temperature of high pressure cell of the Micromeritics Autopore® is not controllable).

The derivative of the intrusion curves $-dV_{Hg}/dE$ are shown in **Fig.6**. Such curves may represent the true PSD provided the porosity is actually made up of slits with parallel faces. The major feature of the PSD of primary A3 consists in a peak centred about $0.012\mu\text{m}$, that accounts for roughly 50% of the total open porosity (compare the E scales in with **Fig.5** and **Fig.6**). This peak narrows slightly and its mode shifts towards larger openings around $0.017\mu\text{m}$, after one or more H-D cycle. The reproducibility of these changes when going from A3P to A3S is made visible in the differential graph $-dV_{Hg}/d\log E$ versus $\log E$ (**Fig.7**) which

includes the results of all experiments. Some physically inconsistent (negative) values of the PSD of the A3S samples may be obtained in the range 0.006-0.003 μm , but this clearly is in relation with the limited accuracy of the intrusion measurement and blank corrections at the highest pressures (the temperature of high pressure cell of the Micomeritics Autopore® is not controllable).

Close examination of the porograms of all samples on the large opening width side and of the corresponding range in **Fig.7** reveals an additional weak and broad component with a mode around 1-2 μm and intensity about two orders of magnitude lower than that of the major peak. Even though it accounts for half the overall open porosity, it contributes practically nothing to the total internal surface area. It can also be concluded that all macropores and mesopores with opening larger than 0.1 μm formed by primary dehydration remain essentially unaffected by successive H-D cycles.

According to Rootare and Prenzlou [14], the surface area of the pore space actually intruded by mercury is related to the integral pressure work by: $S_{MIP} = \sum P \delta V_{p,sp} / \gamma_{Hg} \cos \theta$ where γ_{Hg} is the surface tension of mercury and θ its contact angle with the solid surface. The experimental mean values of $\sum P \delta V_{p,sp}$ and S_{MIP} are reported in **Tab.1** assuming $\gamma_{Hg} = 0.484 \text{ N.m}^{-1}$ and $\theta = 130^\circ$ (the usual default value when direct measurement are missing as in the present case). In computing the integral pressure work, the last 2 to 4 points of the porograms (typically in the pressure range 300-400 MPa) are rejected because they give rise to very high, physically inconsistent, surface area values. In most cases the selection of these values is straightforward because there is a sharp change in the slope of the curves $\sum P \delta V$ -vs- P .

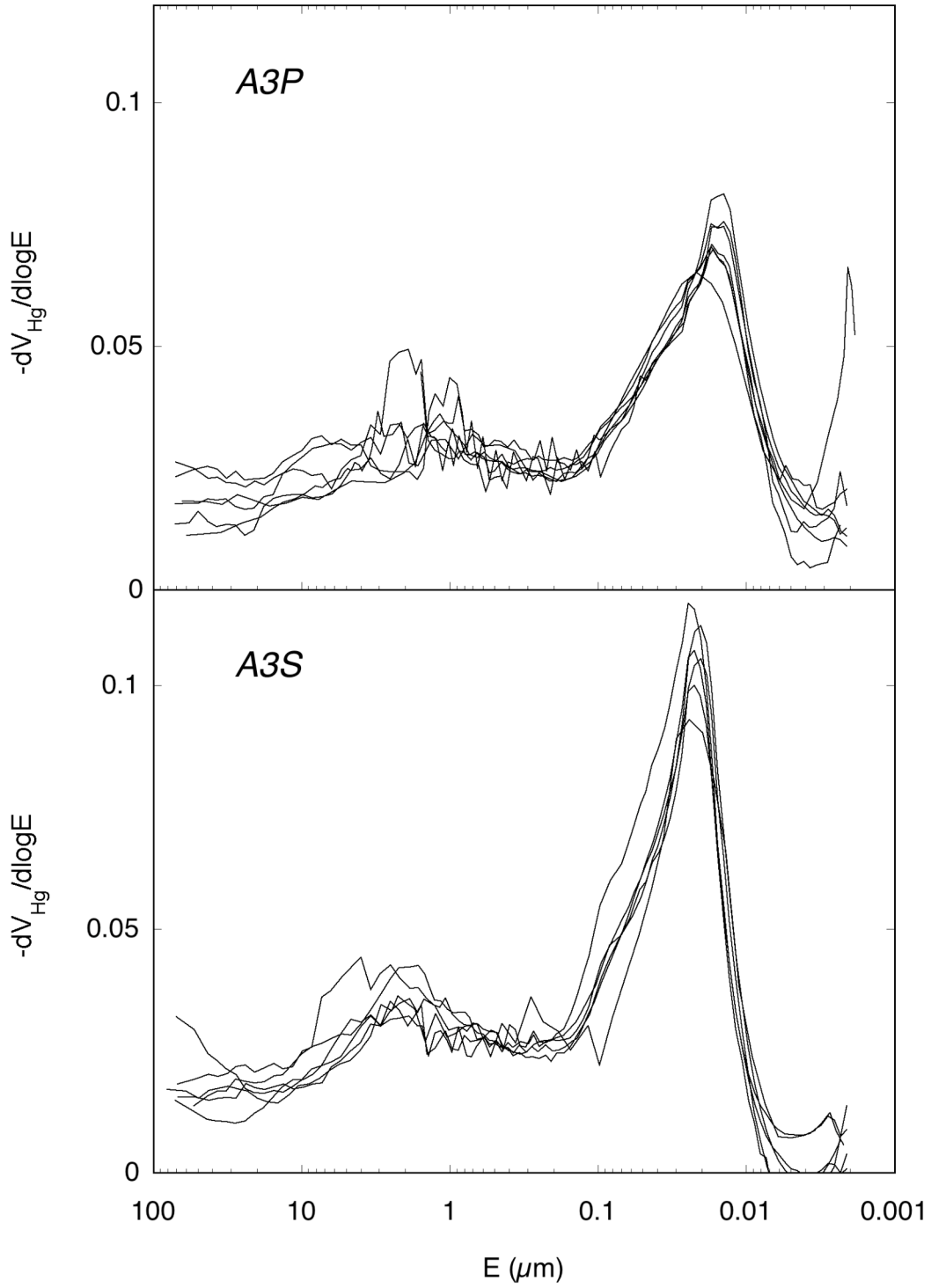


Fig.7: Comparison of the differential porograms $-dV_{\text{Hg}}/d\ln E$ of all measured A3P and A3S samples.

Another way to look at these results is to regard the contact angle of mercury on CaSO_4 as the unknown and estimate its value from $\cos \theta \approx -\sum P \delta V / \gamma_{\text{Hg}} S$. When dealing with the partly

microporous primary anhydrite samples, S must be set equal to S_{EXT} that is to the surface area of the sole mesopores and macropores actually intruded by mercury. As for the A3S samples, S_{BET} is the relevant parameter. Remarkably enough the value $\theta = 131^\circ$ obtained for A3P is very close to the usual default value. The value for A3S samples is slightly larger, but here again the difference is statistically not significant.

4. Discussion

The values of the surface area of primary anhydrite observed in the present work (following dehydration and prolonged equilibration under high vacuum) are essentially invariant around $20 \text{ m}^2 \cdot \text{g}^{-1}$ within the investigated range of dehydration temperatures. As shown in appendix, this is at variance with comparable data from the literature [7,8,10,15,16]. We believe that the highly variable influence of temperature reported in these publications, especially for reactions carried out under vacuum, reflects transitory non-equilibrium microstructural states of the pseudomorphs due to the short isothermal treatments and/or high heating rates imposed.

The experimental adsorption isotherms and t-plots of primary anhydrite in **Fig.1** and **Fig.4** are not representative of a purely either microporous or mesoporous solid (characterized by type I and IV isotherms respectively) but instead of a mixed porosity made up of micropores, mesopores and macropores. The wall surface area of the mesopores and macropores constitutes the external surface area defined by the upper branch of the t-plots. A small positive upward deviation from linearity (convexity) of the t-plot is only observed above 1.5 nm i.e. for $P/P_0 > 0.90$, and we may formally conclude thereof that there is no evidence of capillary condensation at lower partial pressures. This and the shape of the hysteresis loop rules out the presence of cylindrical mesopores with radius lower than about 10 nm and we assume a model of predominantly slit-shaped and/or wedge shaped pores in the mesopore size range.

This and the results of the MIP experiments strongly suggest that the microstructure of a primary anhydrite pseudomorph is comprised of a *continuous* distribution of such pores with opening sizes ranging over about 5 decades and with the same morphology observed by SEM and optical microscopy for macropores in [1, 2] .

According to the IUPAC subcommittee on “Reporting Gas Adsorption data” the very thin hysteresis loop observed in the present work and in [3], is of type H3 which may not bear consistent information about the porous microstructure [13]. Rather, it might reveal some swelling of a loose packing of plate-like particles giving rise to slit-shaped pores *open on all sides*.

On the contrary, if the porous pseudomorph is sufficiently rigid, an increasing fraction of the distribution of slits in the proper nanometer width range should be gradually filled-up by adsorption (pore blocking) and a physically sound PSD could in principle be computed from the desorption branch of the isotherm only [17]. But then, the adsorption t-plot should present some concavity (be lightly bent towards the t axis) and this was not verified experimentally. One possible explanation (that remains to be equated) could be that capillary condensation on curved internal surfaces or along the bottom line of wedge pores compensates more or less exactly for the pore blocking of slits. It may be mentioned that the PSD in clay materials such as montmorillonite and kaolinite have been modelled with some apparent success based on a combination of cylindrical and slit-shaped pores [18] but that no direct evidence of the presence of cylindrical pores was presented.

SEM observations and the mechanical resistance of the pseudomorphs (they can withstand the hydrostatic pressure imposed in MIP experiments without crushing) demonstrate that they are not just loose aggregates of platelets. Instead, the cracks seem to have finite opening length [1,2] and they probably fit in a more realistic model of either wedge pores or slits with a wedge end. The consequence of wedge morphology on *multilayer* nitrogen vapour adsorption has been theoretically studied by Cheng and Cole [19] . It appears

that the equilibrium liquid-vapour interface along the *bottom line* (oblique corner) is curved, which requires an adsorbed volume in excess of that adsorbed on a flat surface. This might account for the apparent capillary condensation at $P/P_0 \geq 0.9$, without resorting to hypothetical cylindrical pores as in [18]. To the author's knowledge the combination of the model of Cheng and Cole with a computational method of the BJH type for obtaining a PSD of such wedge slits remains to be developed and validated. These considerations also explain why the standard BJH method is not employed in the present work to infer some PSD of the mesopores.

As mentioned in the introduction, observations of a strong decrease of the BET surface area of β -anhydrite, following vapour phase rehydration, have been already reported in the literature. The usual experimental procedure, and in particular that reported by Ball [6] (gypsum dehydration in air, surface area measurement by nitrogen adsorption directly on hemihydrate samples not previously dehydrated) are questionable with regards to the actual composition of the analysed solids. Also, the nitrogen adsorption-desorption isotherms on the (α and β) hemihydrate samples (Fig.1 and 2 in [5]) exhibit a *very pronounced low-pressure hysteresis* that either signals a fundamental property of the pseudomorphs or may shed doubts about the experimental procedure used and the results so obtained. In comparison, Ridge and Molony [8] did *not* observed low pressure hysteresis with nitrogen but reported hysteresis loops of *variable shape*, associated in two instances with low pressure hysteresis, in the adsorption of *oxygen* on β -A3 and on β -HH dehydrated at or above 100°C. We also observed low pressure hysteresis in the nitrogen adsorption-desorption isotherms of primary A3 (**Fig.1**), but its amplitude varied with the adsorption equipment used and the total duration of the adsorption experiment. As a general rule, the reality of low-pressure hysteresis is difficult to ascertain experimentally and the microstructural information (if any) carried by the phenomenon hard to decipher. One of the present authors already observed very large low

pressure hysteresis in the adsorption of nitrogen on magnesium stearate at liquid nitrogen temperature using the same Quantachrome and Micromeritics adsorption equipment as in the present work [20].

The description and full understanding of the phenomenon would require specific investigation based on adsorption experiments carried out at different temperatures and/or with various adsorbates and this is beyond the scope of the present investigation.

The other experimental results reported in section 3 are based on unbiased experimental procedures and the consequences of H-D cycles on the microstructure inferred thereof are unquestionable. They can be summarised as follows:

- a) The surface area is strongly reduced and the micropores disappear as primary A3 is submitted to the first H-D cycle (we understand the very small concavity of the t-plots of A3S in the range $0 < t < 1\text{nm}$ as due to the blocking of the finest residual mesopores by adsorption).
- b) The pore size distribution assessed by MIP is also significantly modified in a narrow range of mesopore sizes only. In contrast, the total volume of macropores and of the largest mesopores generated by the primary dehydration remains unchanged (within the limit of accuracy of the method, and taking into account the variable contribution of some large macropores initially present in the cleft gypsum blocks).
- c) The small additional decrease of the surface area resulting from subsequent H-D cycles is at variance with the results of Molony et al. [9]. The surface area values of their β -HH samples degassed at RT were smaller than those observed in the present work and *increased* weakly and somewhat erratically between 1.6 and $3.3\text{ m}^2\cdot\text{g}^{-1}$ over the series of H-D cycles (Tab. 2 in [9]). Notice that the investigated material had been stored for 7 years under 65% RH (which means that $\text{HH}_{0.6}$ must have been formed) and had been incompletely dehydrated at 150°C prior to measurement. Hamad [10] also observed a very low limit value around $1\text{ m}^2\cdot\text{g}^{-1}$ after prolonged rehydration carried out under water *saturated* atmosphere. Here again

the conditions were such that formation of $\text{HH}_{0.6}$ but also water vapour condensation must have taken place. This may point to the fact that some restructuring or recrystallisation of the surface is taking place and is enhanced under high water vapour partial pressure in relation with the reaction $\text{HH}_{0.5} \rightarrow \text{HH}_{0.6}$ and with the presence of thick liquid layer

The present and other results [1, 2] show that the porosity of primary anhydrite is made up of essentially elongated cracks whose orientations with respect to the crystal structure of gypsum have been described and related to the topotactic orientations relations. These microstructural characteristics follow from the anisotropic atomic rearrangements involved in the change of structure. The most frequently observed set of orientation relations [21] involves a contraction as large as 38.6% along direction [010], an expansion of 16,1% along [100] and practically no change along [001] (the directions are indexed in the gypsum structure). Obviously the resulting structural volume decrease, about 28.5%, is almost entirely accommodated by the internal porosity of the anhydrite pseudomorph which is found equal to 26.4 (± 1.7)%. One may conclude that there is no or only a very slight contraction of the initial gypsum crystal habit associated with primary dehydration and that the observed invariance of $V_{a,sp}$ (see **Tab.1**) is evidence that a pseudomorph does *not* swell or shrink along subsequent H-D cycles. In contrast, only minor atomic rearrangements are involved in the transformation $\text{A3} \rightarrow \text{HH}$. They are accompanied by a minute *increase* in molar volume (about 0.5%), but the orientation relationships between the two structures have not been established. Nonetheless, it can safely be assumed that this small volume increase results from the expansion of the primary A3 lattice in at least one direction. It is proposed here that this might be what brings about the closure of the micropores and finest mesopores to the point where the *continuity of the atomic structure is restored*. In the next dehydration step, the mechanical stresses resulting to the reverse atomic rearrangement would be much lower than those

generated in the primary dehydration of gypsum and unable to regenerate the cracks and their associated internal surface area.

5. Conclusion

The work described in the present paper has yielded a combination of experimental data that had never been reported before regarding the materials under consideration. Except for a few points, the general prior knowledge about the microstructure of the pseudomorphs A3P and A3S is not challenged but is largely complemented by new quantitative correlations between nitrogen adsorption and MIP experimental results as summarised in Table 1.

The influence of water vapour reaction and adsorption on CaSO_4 internal surfaces generated by the dehydration gypsum crystals has been investigated in ambient conditions thus avoiding high and very high relative humidity levels (such as larger than 80-90%RH). Our analysis of the literature in the light of the present results indeed suggests that multilayer adsorption at so high relative humidity may create local surface conditions such that the microstructure of the soluble adsorbants A3 and HH be profoundly modified by re-crystallization. Research is under way to clarify this point by revisiting the adsorption-reaction of water on the pseudomorphs.

Appendix

Surface area values of primary anhydrite obtained in the present work and by various other authors are compared in **Fig.8**. Only the experiments of adsorption of nitrogen vapour at 77K have been taken into consideration. Adsorption of another molecular species, namely oxygen in [7, 8], raises several unanswered questions and no clear microstructural picture emerges from its comparison with nitrogen adsorption.

In the range 100-200°C all reported data relate to the soluble anhydrite phase A3 with one exception. In [15] the dehydration of gypsum (a fine powder) and the adsorption of nitrogen on the dehydration product are carried sequentially within a thermobalance, and the pure A3

phase, i.e. complete dehydration, is obtained at 176°C only. The surface area at that temperature reaches the highest value of 36.9 m².g⁻¹. The change of structure of the dehydration product from A3 to A2 is reported around 350°C in [7], 325°C in [15] and 280°C in [16]. It goes with a second maximum in the curves.

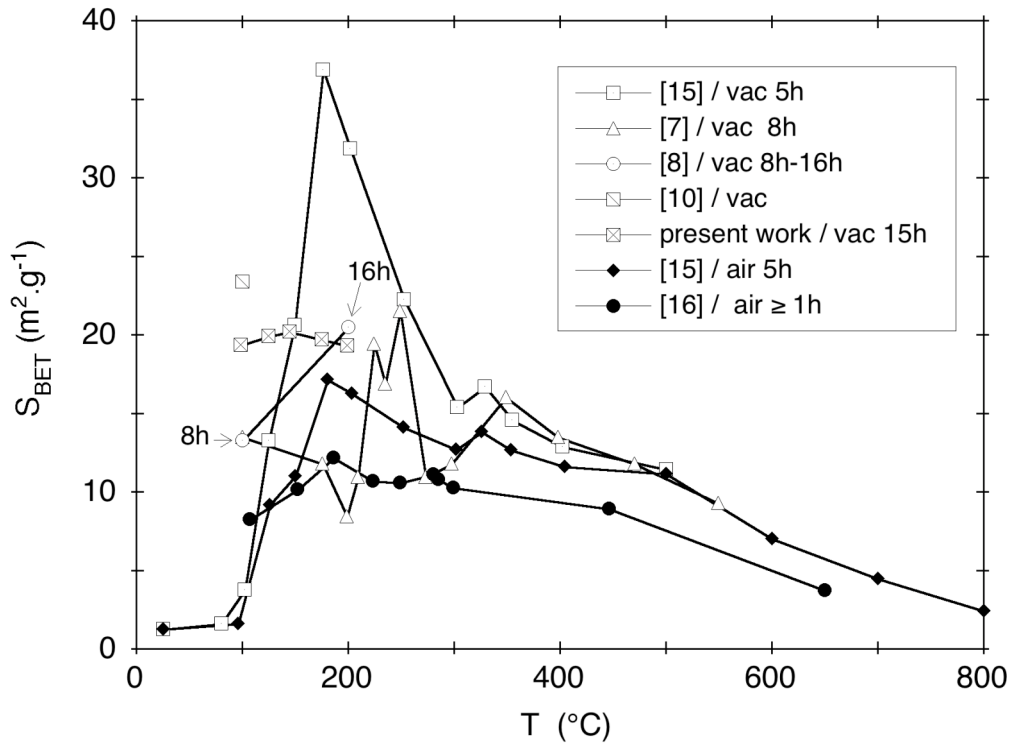


Fig.8: Dependence of the S_{BET} values of the dehydration product of gypsum taken from literature and the present work on the temperature of the isothermal treatment. The duration of the later (expressed in hours) is mentioned.

References

- [1] E.M. Sipple, Doctorate Thesis, University of Burgundy, 1999.
- [2] E.M. Sipple, P. Braconni, P. Dufour, J.-C. Mutin, Solid State Ionics 141-142 (2001) 447.
- [3] C. Bezou, A. Nonat, J.-C Mutin, A. Norlund Christensen, M. Lehmann, J. Sol. State Chem. 117 (1995) 165.

- [4] M. Ball, L. Norwood, *J. Chem. Soc. Faraday Trans.* 73 (1977) 932.
- [5] M. Ball, L. Norwood, *J. Chem. Soc. Faraday Trans.* 74 (1978) 1477.
- [6] M. Ball, *Brit. Ceram. Trans. J.* 88 (1989) 79.
- [7] B. Molony, M.J. Ridge, M. Goto, *J. Chem. Soc. A* (1966) 864.
- [8] M.J. Ridge, B. Molony, *Trans. Faraday Soc.* 65 (1969) 1113.
- [9] B. Molony, J. Beretka, M.J. Ridge, *Aust. J. Chem.* 24 (1971) 449.
- [10] S. Hamad, *Trans. Brit. Ceram. Soc.* 80 (1981) 51.
- [11] S. C. Williams, *Tectonophys.* 148 (1988) 163.
- [12] J.D.C. Mc Donnell, *Mineral. Mag.* 34 (1965) 327.
- [13] K. Sing, D. Everett, R. Haul, L. Moscou, R. Pierotti, J. Rouquérol, T. Siemienka, IUPAC, *Pure Appl. Chem.* 57 (1985) 603.
- [14] H.M. Rootare, C.F. Prenzlów, *J. Phys. Chem.* 71 (1967) 2733.
- [15] D.R. Glasson, P. O'Neill, *J. Appl. Chem.* 17 (1967) 102.
- [16] S.J. Gregg, E.J. Willing, *J. Chem. Soc.* (1951) 2373.
- [17] J.C.P. Broekoff, B.G. Linsen, in: B.G. Linsen (Ed.), *Physical and Chemical Aspects of Adsorbents and Catalysts*, Academic Press, London, 1970, p. 39.
- [18] S.D. Christian, E.E. Tucker, *Int. Laboratory* 12 (1982) 40.
- [19] E. Cheng, M.W. Cole, *Phys. Rev. B* 41 (1990) 9650.
- [20] C. Andrès, P. Bracconi, Y. Pourcelot, *Int.J. Pharm.* 218 (2001) 153.
- [21] E.M. Sipple, P. Bracconi, P. Dufour, J.-C. Mutin, *Solid State Ionics* 141-142 (2001) 455.

Table 1: Mean and standard deviation values of various descriptors of the porosity and surface area for all analysed samples, regardless of the difference in dehydration temperature or number of H-D cycles. The number of independent measurements is 7 for primary A3 and 6 for cycled A3 samples, except where otherwise stated (numbers between brackets).

	Primary A3	Cycled A3
$V_{a,sp}$ (cm ³ .g ⁻¹)	0.570 (±0.028)	0.578 (±0.038)
$V_{p,sp}$ (cm ³ .g ⁻¹)	0.150 (±0.009)	0.147 (±0.009)
$\rho^{(1)}$ (g.cm ⁻³)	2.38 (±0.21)	2.32 (±0.25)
Open porosity (%)	26.4 (±1.7)	25.9 (±1.3)
Closed porosity ⁽²⁾ (%)	≈ 5.0 (±7)	≈ 6.9 (±9)
$\sum P\delta V_{p,sp}$ (Pa.m ³ .g ⁻¹)	4.45 (±0.95)	2.57 (±0.53) [4 values]
$S_{MIP}^{(3)}$ (m ² .g ⁻¹)	14.3 (±3.1)	8.26 (±1.7) [4 values]
S (m ² .g ⁻¹)	14.25 (±0.25) [5 values]	5.75 (±0.22) [4 values]
$\theta = \cos^{-1}\left(-\sum P\delta V_{p,sp} / \gamma_{Hg} S\right)$	131° (±8°)	137° (±10°)

(1) $\rho = 1/(V_{a,sp} - V_{p,sp})$

(2) $V_{a,sp} - V_{p,sp} - 1/\rho_{X-ray}$ using $\rho_{X-ray} = 2.556 \text{ g.cm}^{-3}$ as density value for A3

(3) with $\gamma_{Hg} = 0.484 \text{ N.m}^{-1}$ and $\theta = 130^\circ$